Marine and Petroleum Geology
July 2021, Volume 129, Pages 105094 (9p.)
https://doi.org/10.1016/j.marpetgeo.2021.105094
https://archimer.ifremer.fr/doc/00690/80241/

Archimer
https://archimer.ifremer.fr

The organic, inorganic and isotope geochemistry of the Holocene sapropel units in the Sea of Marmara and their Paleoceanographic significance

Liu Yingjia [1, 2], Lu Xindi [2, 3], Çağatay M.Namık [4], Zhang Yixuan [2, 3], Li Yuanyuan [1, 2], Peng Yongbo [5], Ruffine Livio [6], Lu Hailong [2, 3, *]

[1] College of Engineering, Peking University, Beijing 100871, China
[2] Beijing International Center for Gas Hydrate, Peking University, Beijing 100871, China
[3] School of Earth and Space Sciences, Peking University, Beijing 100871, China
[4] EMCOL Research Centre, Istanbul Technical University, Istanbul, Turkey
[5] Department of Geology and Geophysics, Louisiana State University, Baton Rouge, Louisiana 70803, USA
[6] Ifremer, Département Ressources physiques et Ecosystèmes de fond de Mer (REM), Unité des Géosciences Marines, Laboratoire des Cycles Géochimiques et ressources (LCG), 29280 Plouzané, France

* Corresponding author : Hailong Lu, email address : hlu@pku.edu.cn

Abstract :

The ocean redox structure and nitrogen utilization are investigated in the Holocene sapropel depositions in the Sea of Marmara, based on inorganic, organic, and isotopic analyses and grain-size distribution of the sediments of a piston core from Çınarcık Basin. Two sapropel units are identified in the core studied, the lower (main) sapropel of the early Holocene and the upper sapropel of the middle-late Holocene. Relatively high C/N ratios (10-11) and smaller δ13Corg values (~ -26‰) in the lower Holocene sapropel unit indicate that the organic matter is mainly of terrestrial origin. Up to 5.5‰ δ15N values and Mo concentration (6.5 ppm) above crustal values in the bottom of the lower sapropel unit strongly suggest that bottom-water conditions were denitrifying and suboxic-dysoxic, suitable for the preservation and burial of the organic matter. Such bottom-water conditions were induced by water stratification that resulted from the transgression from the Aegean Sea coupled with a riverine influx from the Black Sea that provided the terrestrial organic matter. A progressive upward decrease of C/N ratios and increase of δ13Corg values in the upper sapropel unit might have been caused by the additional supply of organic matter of mainly marine origin and improved ventilation of the lower water, which resulted in the oxidation of the organic nitrogen pool and a decrease of δ15N values (below 3‰) under nitrate-rich conditions. Mn enrichment in the upper sapropelic sediments also supports a relatively oxidative environment.

Please note that this is an author-produced PDF of an article accepted for publication following peer review. The definitive publisher-authenticated version is available on the publisher Web site.

Highlights

► Nitrogen isotopic compositions in the Holocene sapropels from the Sea of the Marmara are reported for the first time. ►The redox condition changed from suboxic-dysoxic to relatively oxidative during the Holocene sapropel deposition. ►The nutrition condition shifted from low nitrate to temporally nitrate-rich during the sapropel deposition. ►Holocene sapropel deposition in the Sea of Marmara was closely related to the regional paleo-hydrological condition.

Keywords : Sea of Marmara, Holocene sapropel, Ocean redox structure, Nitrogen utilization, Organic matter sources

Please note that this is an author-produced PDF of an article accepted for publication following peer review. The definitive publisher-authenticated version is available on the publisher Web site.

Journal Pre-proof

1 Introduction

Sapropels typically contain organic carbon concentrations between 1 and 10 wt.%, which contrast with surrounding organic-depleted sediments (Çağatay et al., 2019; Rohling et al., 2015). Sapropel formations have formed repeatedly in the Mediterranean, the Sea of Marmara, and the Black Sea, in response to the variations of solar radiation/global and regional climatic patterns/monsoon runoff (Bahr et al., 2005; Dirksen et al., 2019; Grant et al., 2016; Grimm et al., 2015; Rohling et al., 2015). In the Sea of Marmara (SoM), sapropels are sediments containing more than 1.5 wt.% organic carbon (Çağatay et al., 1999; Çağatay et al., 2009; Çağatay et al., 2000; Çağatay et al., 2015; Sperling et al., 2003; Tolun et al., 2002). Two sapropel units, the main Holocene (lower) and the Middle-Late Holocene (upper) sapropels, were detected in the SoM during the Late Glacial-Holocene period, which are radiocarbon dated at 12.3-5.7 kyr BP and ca. 5.4 and 2.7 kyr BP, respectively (Çağatay et al., 2015). The onset of the main Holocene sapropel deposition is 1.5 ka older than sapropel S1 in the Mediterranean that started forming at 10.8 cal. ka BP (De Lange et al., 2008).

Several factors have been involved in explaining the sapropel formation in the Mediterranean, the Black Sea, and Sea of Marmara: a. increased influx of terrestrial organic matter and freshwater, which contribute to the onset of the sapropel formation (Aksu et al., 1999; Bouloubassi et al., 1999; Çağatay et al., 1999; Çağatay et al., 2000; Checa et al., 2020; Tolun et al., 2002; Vidal et al., 2010); b. enhanced surface ocean productivity and export of organic matter to sediments (Calvert and Fontugne, 1987; Calvert et al., 1992; Sperling et al., 2003); c. suboxic/anoxic conditions resulting from a large influx of freshwater/marine flooding/enhanced monsoon intensity (Benkovitz et al.,

2020; Çağatay et al., 2019; Çağatay et al., 2000; De Lange et al., 2008; Möbius et al., 2010; Moodley et al., 2005; Rohling et al., 2015); d. combination of increased production and better preservation of organic matter (Bouloubassi et al., 1999; Çağatay et al., 2009; Checa et al., 2020; Higgins et al., 2010; Lane-Serff et al., 1997; Tolun et al., 2002; Triantaphyllou et al., 2014; Vidal et al., 2010); e. precession-controlled atmospheric temperature variability (Dirksen and Meijer, 2020; Triantaphyllou et al., 2014). However, the relative importance of these factors for sapropel formation is still being debated, and conflicting interpretations are often invoked. To clarify the major factors involved in the sapropel formations in the SoM, nitrogen isotopes have been used to infer nutrient utilization and sapropel-forming redox condition.

Nitrogen is an essential macronutrient to all life, establishing linkages between ocean redox, nutrient supply, and organic productivity (Ader et al., 2014; Francis et al., 2007; Holmes et al., 1999; Sigman and Casciotti, 2009; Stüeken et al., 2016; Wang et al., 2018b). Nitrogen involves numerous oxidation states, molecular diversity, and microbial typologies (Canfield et al., 2010). Physical, chemical, and biological process discriminates between ^{14}N and ^{15}N, leading to measurable differences in the $\delta^{15}N$, making it a powerful tracer of oceanic processes (Ader et al., 2014; Robinson et al., 2012; Sigman and Casciotti, 2009). Nitrogen enters the marine N cycle mainly through fixation of the atmospheric N_2 with minor isotopic fractionation (≤2‰) (Sigman and Casciotti, 2009). Denitrification and anaerobic ammonium oxidation release nitrogen back to the atmosphere as N_2O or N_2, which only occurs under low-oxygen conditions (Francis et al., 2007; Sigman and Casciotti, 2009). Denitrification (reduction of NO_3^- to N_2) causes a significant fractionation of ~20‰ in the water column, whereas the same process leads to a negligible fractionation within

sediments (Brunner et al., 2013; Sigman and Casciotti, 2009; Stüeken et al., 2016). The balance between nitrogen fixation and denitrification/anammox ultimately governs the inorganic nitrogen reservoir in the ocean and its isotopic composition (Montoya and Voss, 2006; Sigman and Casciotti, 2009). The nitrogen isotope composition of sedimentary organic matter has excellent potential to provide clues about paleoceanographic nutrient conditions and redox structure (Ader et al., 2014; Higgins et al., 2010; Robinson et al., 2012; Stüeken et al., 2016). Phototrophic organisms can utilize various forms of dissolved nitrogen species to produce biomass, which is then deposited in the sediments and preserved through geological time. Thus, the sedimentary sequence theoretically records the history of surface ocean processes (Higgins et al., 2010; Sigman and Casciotti, 2009; Wei et al., 2016).

Up to now, there are only a few studies that have been conducted to reconstruct the paleoceanographic nutrient/productivity conditions and redox structure during the sapropel deposition using nitrogen isotopes of sediment from the Holocene sapropels in the adjacent Black Sea and Mediterranean (Calvert et al., 1992; Higgins et al., 2010; Möbius et al., 2010). In the Sea of Marmara, there is almost no published $\delta^{15}N$ data on the sapropels to constrain the marine redox conditions.

The main focus of this study is to improve our understanding of the major factors controlling the formation of sapropels in the SoM. Nitrogen isotopes, combined with the determination of two redox-sensitive element contents, Mo and Mn, are used to trace the variation in the marine redox conditions. C/N ratios and stable carbon isotopic signatures of organic matter are measured to define the contributions of marine and terrigenous organic matter to the two Holocene sapropel units. In addition, grain size distribution is

112 used to infer changes in physical sedimentary conditions during the sapropel formation.
113 The results are discussed in terms of possible links between ocean redox structure, nutrient
114 cycling, and primary productivity.

115 2 Materials and analytical methods

116 The sea of Marmara connects the Black Sea to the north and the Mediterranean to
117 the west through the straits of Bosphorus (sill depth: ~ -35 m) and Dardanelles (sill depth: ~
118 -65 m), respectively (Çağatay et al., 2009; Çağatay et al., 2000; Kirci-Elmas et al., 2008).
119 Thus, the SoM is influenced by two important water masses, leading to a two-layer water
120 stratification. The upper water layer originates from the Black Sea and has a salinity of ~22
121 psu, whereas the lower layer is saltier (~38 psu) and denser supplied from the
122 Mediterranean. The Çınarcık Basin is the broadest and deepest basin (1275m deep) in the
123 SoM and has a sedimentation rate of 1-3 m/kyr during the Holocene (Çağatay et al., 2012;
124 Çağatay et al., 2009; Çağatay et al., 2000; Liu et al., 2019). The studied gravity core
125 MRS-CS17 was collected from this basin (N 40° 42.9884, E 29° 6.7063) during the
126 MARSITE cruise expedition onboard the R/V *Pourquoi pas?* in November 2014 (Figure
127 S1). This 1038 cm long core was cut into 1m-length sections, and each section was split
128 lengthwise into two half cores and systematically sub-sampled with a resolution interval of
129 ~30 cm.

130 AMS radiocarbon analyses on organic carbon in high total organic content (TOC)
131 intervals were carried out at Beta Analytic Inc. in Florida. The ^{14}C ages of organic carbon
132 were calibrated to calendar ages with the INTCAL13 calibration curve (Reimer et al.,
133 2013). A reservoir age of 400 years for the marine unit was used for the calibration,

Journal Pre-proof

assuming that only organic matter of marine origin was present in the analyzed samples (Çağatay et al., 2015; Siani et al., 2000; Soulet et al., 2011).

The isotopic analyses of nitrogen ($\delta^{15}N$) and organic carbon ($\delta^{13}C_{org}$), together with total nitrogen (TN), and total organic carbon (TOC) were carried out in the Oxy-Anion Stable Isotope Consortium (OASIC) at the Louisiana State University (LSU). Aliquots of powdered samples between 20 and 50 mg were decarbonated with 12M hydrochloric acid (HCl). Then deionized water (18.2 MΩ) from Milli Q was used to rinse the powders until the pH reaches 4-5. Subsequently, the samples were dried and wrapped in tin capsules prior to analysis. The analyses were performed using Vario Microcube Elemental Analyzer (EA) connected to an Isoprime 100 isotope ratio mass spectrometer (IRMS). $\delta^{15}N$ results are reported in per mil relative to atmospheric N_2. Uncertainties are better than 0.3‰ for $\delta^{15}N$ and 0.08% for TN. $\delta^{13}C_{org}$ values are reported in per mil deviations from VPDB. Analytical reproducibility is better than 0.2‰ for $\delta^{13}C_{org}$ and 0.3% for TOC.

Molybdenum (Mo) and manganese (Mn) concentrations were measured on a Perkin Elmer NexION 350 ICP-MS at State Key Laboratory of Biogeology and Environmental Geology, China University of Geosciences (Wuhan). The calibration curves were constructed from a series of standard gravimetric solutions with a concentration range of 1-1000 ppb.

Grain size analyses were performed after treatment for removal of carbonate, amorphous metal oxides, and silica at Beijing International Center for Gas Hydrate, using a Malvern Mastersizer S equipment. Mean grain size, sorting, and skewness were determined using the Malvern software.

3 Results

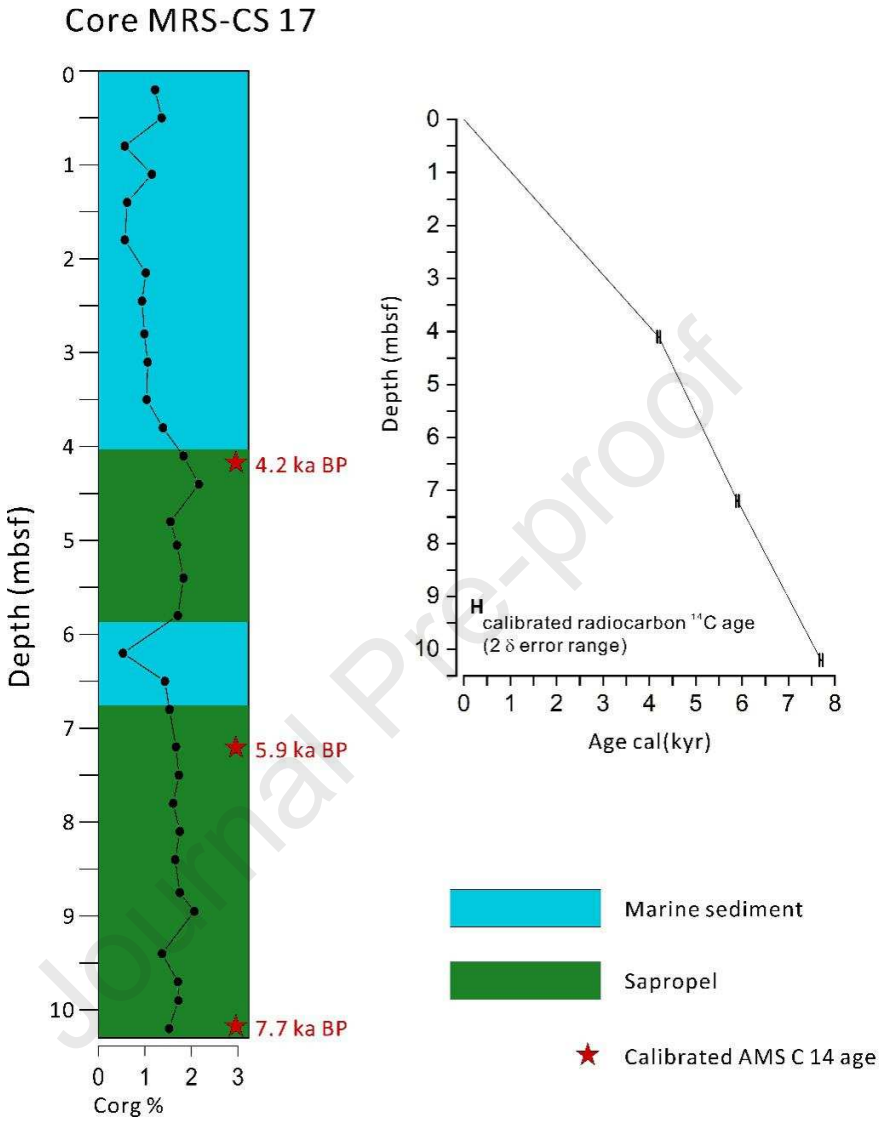

Figure 1. Lithostratigraphy and age-depth model of core MRS-CS 17, based on three AMS radiocarbon ages.

Core/sample	Core Depth (cmbsf)	Calendar age (cal yr BP)	2σ (±yr)
CS 17/ sediment	410	4180	30
	720	5930	30
	1020	7720	30

Table 1. Calibrated AMS ^{14}C ages of organic carbon in sediments from core MRS-CS 17, Sea of Marmara.

Journal Pre-proof

3.1 Chrono-stratigraphy

The age-depth model for the 1038 cm-long core MRS-CS17 is established by three radiocarbon datings of bulk sedimentary organic matter (Fig.1, Table 1). The core comprises only the marine unit, including two sapropel layers, which are defined by their relatively high TOC content (>1.5 wt%) and dark olive green color. Core MRS-CS17 intercepts only part of the main sapropel unit, whose upper boundary is dated at 5.9 kyr BP. The upper sapropel is dated at ca. 5.5-4 cal kyr BP. These two sapropelic layers in core MRS-CS 17 are broadly contemporaneous with the sapropels previously dated by Çağatay et al. (2015) in cores elsewhere in the Sea of Marmara at 12.3 -5.7 cal kyr BP and ca. 5.4 and 2.7 cal kyr BP, respectively.

3.2. Total organic carbon, total nitrogen, and C/N ratio

The upper sapropel is with a slightly higher total organic carbon (TOC), an average of 1.8% compared to the average of 1.7% in the lower (main) sapropel. The lowest TOC content (0.53%) occurs in the interval between the two sapropel units, while intermediate values occur in sediments overlying the upper sapropel (Fig.2a). Total nitrogen (TN) values show a consistent pattern paralleling the TOC trend, with the sapropel units containing relatively high TN contents of 0.14-0.21%. A negative excursion of 0.05% occurs in the interval between the two sapropel units (Fig.2b). In the sediment unit overlying the upper sapropel from 20 to 330 cmbsf, the TN contents display relatively low values with an average of 0.11%.

The C/N ratio varies between 10 and 11 in the lower part of the main sapropel (10.20-8.95 mbsf), after which it decreases slightly from ~10 to ~9.6 in the upper part of the main sapropel unit, except for a positive anomaly of ~11 at ~900 cmbsf (Fig.2c). The

unit deposited between the two sapropel layers is with a relatively high C/N ratio of 11. In the upper sapropel, C/N values show a slightly upward decreasing trend from ~10 to ~9.5. The topmost unit of the core is with C/N values varying between ~8 and ~10.5.

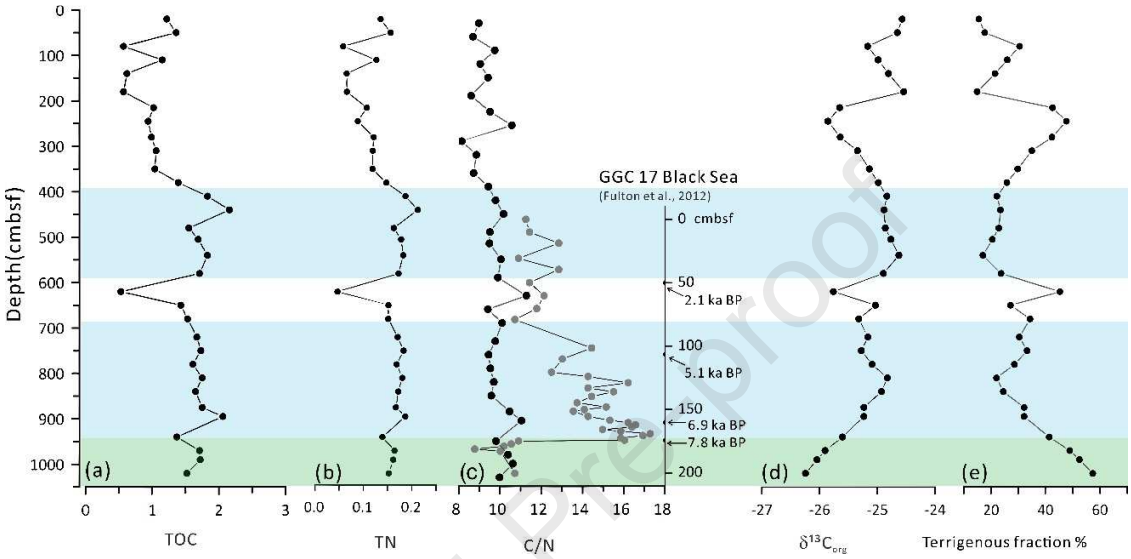

Figure 2. Plots of TOC, TN, C/N, $\delta^{13}C_{org}$, and the terrigenous fraction (%) in core MRS-CS 17, the Sea of Marmara. The upper and lower shaded bands show the middle-late and the main Holocene sapropel units, respectively. The green and blue shades in the main Holocene sapropel indicate the intervals containing organic matter predominantly of marine and terrigenous origin. The solid grey circles in Figure 2(c) represent the C/N ratios from the Black Sea (Fulton et al., 2012).

3.3 Organic carbon isotopes

The organic carbon isotopic ratios ($\delta^{13}C_{org}$) in the interval of 10.20 to 8.10 mbsf of the core show low but upward increasing values ranging from -26.2 to -24.8‰ and averaging at -25.5‰ (Fig.2d). In the upper part of the main sapropel, the $\delta^{13}C_{org}$ values show a slight decrease from -24.8‰ to -25.3‰. The layer between the two sapropels is relatively depleted in ^{13}C with a minimum $\delta^{13}C_{org}$ value of -25.8 ‰ at 6.20 mbsf, which corresponds to the positive excursion in the C/N value. The upper sapropel shows a general slightly upward decreasing trend $\delta^{13}C_{org}$ values ranging from -24.6‰ to -24.9‰. $\delta^{13}C_{org}$

values in sediments overlying the upper sapropel vary within a relatively wide range between -25.9‰ at 2.45 mbsf and -24.5‰ at 1.80 mbsf.

3.4 Nitrogen isotopes

The $\delta^{15}N$ values of different units in core MRS-CS17 range between 2.3 ‰ and 5.5‰ (Fig.3a), approaching typical values for modern sediments (Sigman et al., 2000; Wang et al., 2018a). The main sapropel display two sets of $\delta^{15}N$ values, 3.6-5.5‰ in the interval of 10.20-9.40 mbsf and +2.9‰ in the interval of 8.95-6.80 mbsf. In the upper sapropel (5.80 to 4.10 mbsf), $\delta^{15}N$ exhibit overall smaller values, varying between 2.3 to 2.8‰, except for a scattered high excursion of 3.7‰ at 4.80 mbsf. In sediments overlying those sapropelic layers, $\delta^{15}N$ rise above 3.0‰ with a peak of 5.5‰ at 0.20 mbsf. A notable positive shift of 4.3‰ occurs at 6.20 mbsf between the two sapropelic layers.

3.5 Molybdenum (Mo) and Manganese (Mn) concentrations

Molybdenum and Manganese show sharp changes in different core intervals (Fig. 3b and 3c). High Mo contents above the crustal value (2 ppm) (Taylor and McLennan, 1985) are observed in the lower part of the core in the lower sapropel with 6.5 ppm at 9.70 mbsf and 4.1 ppm at 9.40 mbsf. In the upper part of the main sapropel, the Mo contents exhibit constant values below 2 ppm. Interestingly, in the upper sapropel and in the sediments between the two sapropels, the Mo contents are higher, with several excursions slightly higher than 2 ppm.

Mn concentrations are relatively high below 10 mbsf in the main sapropel, with up to 2270 ppm at the bottom. In the upper part of the main sapropel and the intervening unit between the two sapropels, the concentrations vary between ~1000 and 1500 ppm. Mn concentrations are relatively high in the upper sapropel layer, with a range of ~2500-4510

226 ppm. In the uppermost sediments, the Mn concentration shows high fluctuations between
227 950 to 4150 ppm.

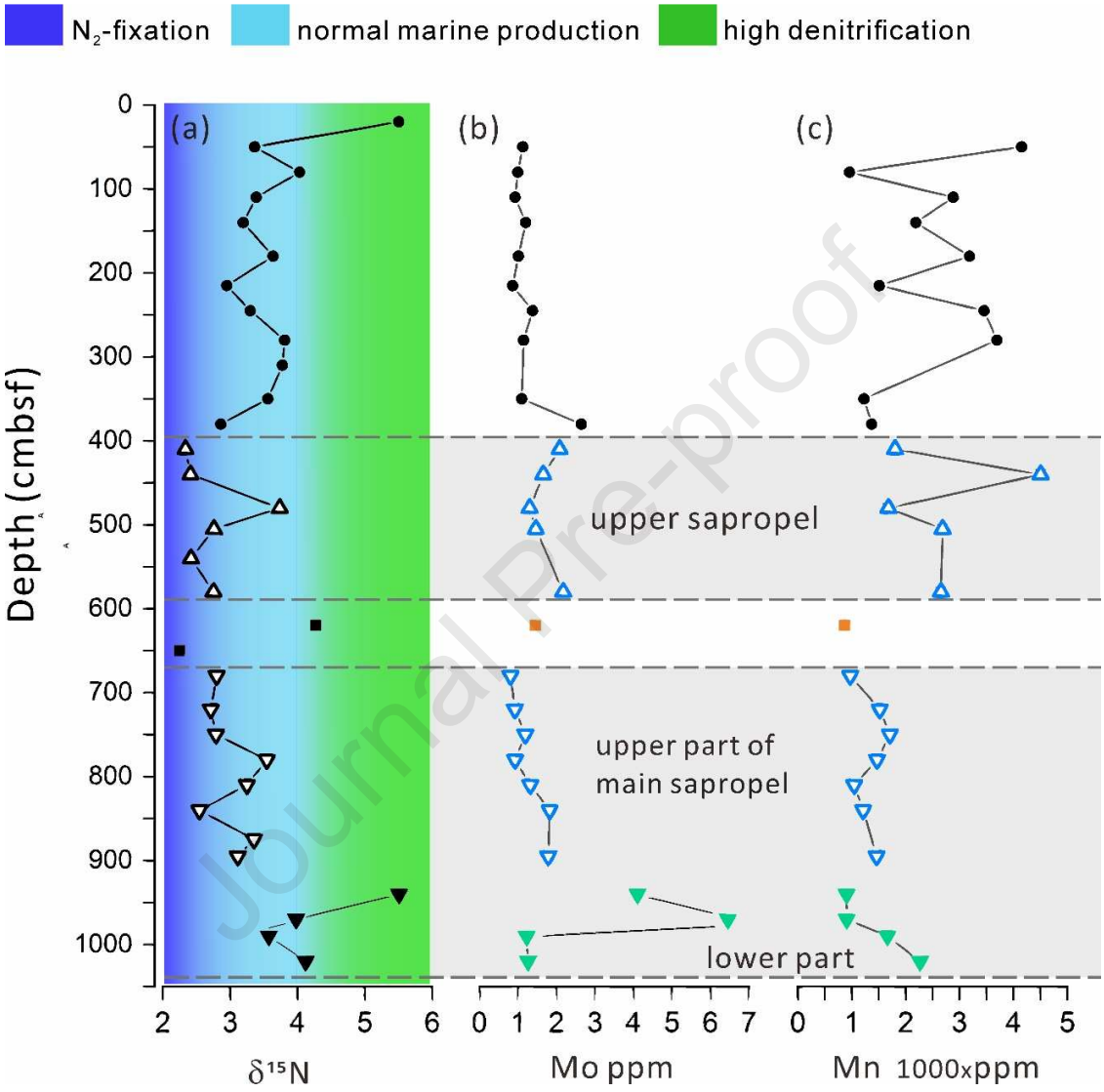

228

229 **Figure 3.** Profiles of (a) $\delta^{15}N$, (b) Mo, and (c) Mn in core MRS-CS 17. Colors imply
230 possible biochemical processes corresponding to nitrogen isotopic fractionation (from
231 Cremonese et al., 2013; see text for explanation). Note the Mo enrichment above typical
232 crustal values of <2 ppm in the lower part of the main Holocene sapropel unit, and relative
233 Mn enrichment in the upper sapropel unit and the recent sediment unit above.

Journal Pre-proof

3.6 Grain-size distribution

The mean grain size of the main sapropel (10.20-6.80 mbsf) is about 9.8 μm, slightly larger than (8.7 μm) in the upper sapropel (Fig.4). There are two silty layers at 6.20 mbsf and 0.80 mbsf in the core, with the grain size of 12.7 μm and 16.4 μm, respectively. Most sedimentary succession shows moderate sorting with the standard deviation between 0.77 and 0.97, except for the silty layers, with the values of 1.19 and 1.38. The skewness values average at ~ -0.4 for the main sapropel, -0.5 for the upper sapropel and the overlying sediments. The two silty samples show skewness values of -0.29 at 6.20 mbsf, and of -0.19 at 0.80 mbsf. There is a weak positive correlation between the TOC and skewness, but no correlation is identified between sorting (standard deviation) and TOC.

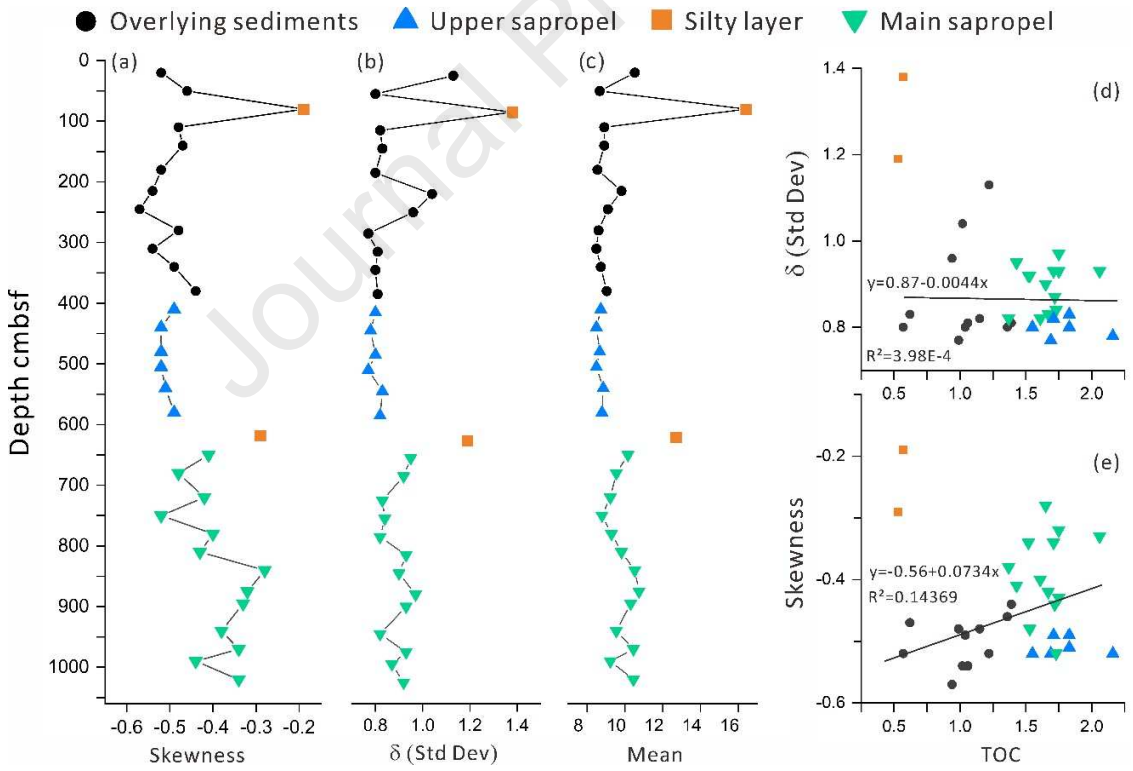

Figure 4. Plots of grain-size parameters in core MRS-CS 17 from the Çınarcık Basin.

Journal Pre-proof

4 Discussion

4.1 Sources of the organic matter in the two sapropel units

4.1.1 Preservation of the organic matter

The use of paleoceanographic proxies such as carbon and nitrogen isotopes and C/N ratios for the sources of organic carbon and redox indicators require certain conditions of no significant post-depositional alteration of the original organic matter and no changes in possible sources of nitrogen. The TN and TOC in the sediments are usually used to characterize the extent of such possible post-depositional alterations (Calvert, 2004; Kikumoto et al., 2014; Wei et al., 2017). TOC and TN in core MRS-CS 17 show a positive linear relationship, with the linear regression line passing almost through the origin (Fig. 5). The strong linearity implies that the organic fraction in the sediments has a uniform composition, and the near-zero intercept on the TN axis indicates that there is little or no clay-bound nitrogen (Calvert, 2004). The lack of a linear correlation between C/N ratios and TOC contents further suggests that no significant loss of organic nitrogen occurred during early diagenesis (Fig. 5).

The cross-plots of $\delta^{15}N$ vs. TN and TOC show the absence of any correlation between these variables in all the sediment units (Fig. 5). These results imply that the early sediment diagenesis, as well as the organic matter degradation during settling through the water column, did not alter the nitrogen isotope composition of the sediments (Calvert et al., 1992; Kikumoto et al., 2014). The overall $\delta^{13}C_{org}$ trends appear to be independent of TOC, indicating that the $\delta^{13}C_{org}$ mainly reflects the source of organic matter (marine vs. terrestrial) (Fig. 5).

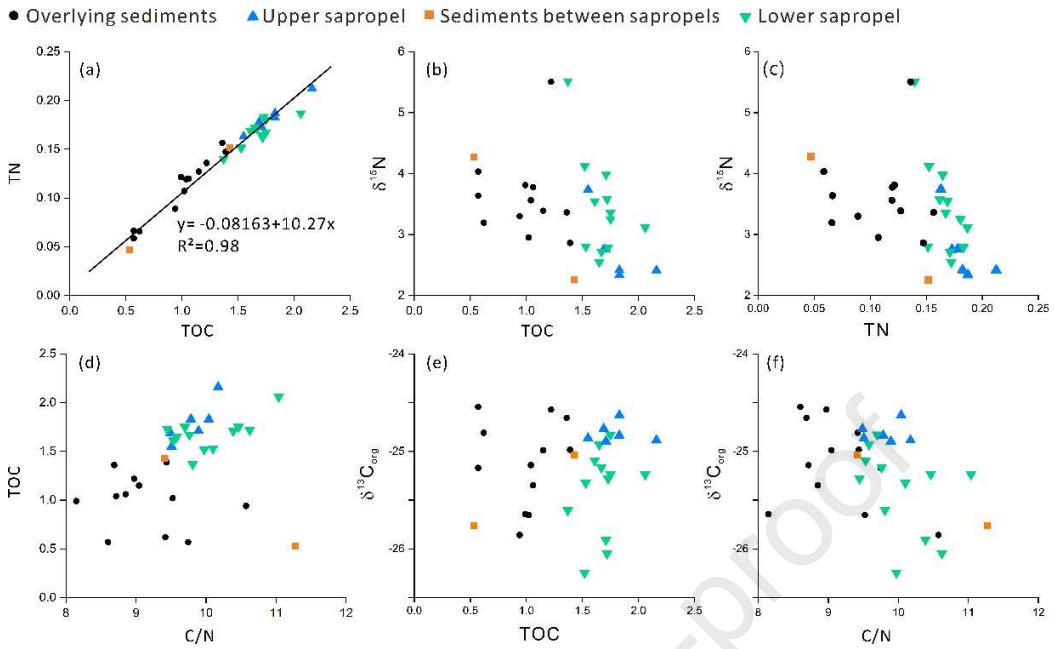

Figure 5. Cross-plots of: (a) TN vs. TOC; (b) $\delta^{15}N$ vs. TOC; (c) $\delta^{15}N$ vs. TN; (d) TOC vs. C/N; (e) $\delta^{13}C_{org}$ vs. TOC; (f) $\delta^{13}C_{org}$vs. C/N of the sediment core MRS-CS 17 from the Çınarcık Basin, the Sea of Marmara.

4.1.2 Sources of the organic matter

The C/N ratios are frequently used to identify the source of sedimentary organic matter (Aksu et al., 1999; Emerson and Hedges, 1988; Tolun et al., 2002). C/N ratios lower than 10 for marine plankton are relatively lower than those for land plants. The organic stable carbon isotope is also routinely used to discriminate between the marine planktonic and terrestrial organic sources (Aksu et al., 1999; Calvert and Fontugne, 1987; Tolun et al., 2002). Variable $\delta^{13}C_{org}$ values in the Marmara core section suggest that the sedimentary organic matter are mixtures of the two end-members (Calvert and Fontugne, 1987). A first-order mixing equation, with $\delta^{13}C_{org}$ of marine and terrestrial sources as two end-members, is used to estimate their contributions (Aksu et al., 1999; Calvert and Fontugne, 1987; Tolun et al., 2002):

Journal Pre-proof

$$\delta^{13}C_{org} = f_{terrestrial} \times \delta^{13}C_{terrestrial} + f_{marine} \times \delta^{13}C_{marine} \quad (1)$$

$$f_{terrestrial} + f_{marine} = 1 \quad (2)$$

where *f* represents the fraction.

The marine end-member is assumed to be -23.95‰ VPDB, which is the value of modern marine plankton in the eastern Mediterranean and the Black Sea (Aksu et al., 1999). The terrestrial end-member is the typical value for the C_3 plants in temperate climatic zones, which is -28.95‰ VPDB (Aksu et al., 1999; Calvert and Fontugne, 1987). In accordance with the relationship in the formulae, the terrestrial fraction profile shows an inverse relationship to that of the $\delta^{13}C_{org}$ (Fig.2e).

Two sapropel units (the main and upper sapropels) were deposited in the latest Pleistocene-Holocene between 12.3 - 5.7 cal ka BP and ca. 5.4 and 2.7 cal ka BP in the Sea of Marmara (Çağatay et al., 2009; Çağatay et al., 2000; Tolun et al., 2002). In the lower portion of the core, the main sapropel layer is associated with obviously higher C/N ratios (10-11) and smaller $\delta^{13}C_{org}$ values (~ -26‰) (Fig.2). These results suggest that terrestrial organic matter plays a relatively more important role in the lower portion than in the upper part of the main sapropel (Aksu et al., 1999; Emerson and Hedges, 1988; Tolun et al., 2002). The first-order estimation results, based on $\delta^{13}C_{org}$ of marine and terrestrial sources as the two end-members, show a terrestrial fraction of 57.4% in the bottom of the core (Fig.2). These results are consistent with previous observations suggesting that the onset of sapropels deposited during early Holocene in the SoM is induced by a high input of terrestrial organic matter (Çağatay et al., 2009; Çağatay et al., 2000; Tolun et al., 2002). The terrestrial organic matter in the main Holocene sapropel was likely provided by organic-laden runoff waters via the European rivers into the Black Sea and from there to the SoM (Çağatay et al., 2009; Çağatay et al., 2000; Tolun et al., 2002) (Fig.6a). This is

supported by the similarity of the C/N values of the Black Sea sediments deposited during the same time interval (Fig. 2c). The onset of the sapropel S1 deposition in the Mediterranean ca. 1.5 ka later was similarly marked by an increase in high-molecular-weight *n*-alkanes showing a significant influx of fresh vascular plant material, as well as the pollen assemblage suggesting the assumption that most of the insoluble organic matter are typical of terrigenous humic compounds (Aksu et al., 1999).

In the upper part of the main sapropel and the upper sapropel deposited during 7-5.7 cal ka BP and ca, 5.4 and 2.7 cal ka BP, the gradual decrease of C/N ratios coincides well with the progressive increase of $\delta^{13}C_{org}$ values, indicating an increase in the proportion of the marine organic matter (Fig.2). The first-order estimation based on $\delta^{13}C_{org}$ values demonstrates that the terrestrial fraction decrease from 32.2% in the main sapropel to 22.2% in the upper sapropel (Fig.2). These results illustrate that marine productivity is the main contributor to the organic matter in the upper sapropel. As also recorded in the Aegean Sea, there is an increase in low-molecular-weight *n*-alkanes from ~8.2 to 6.4 kyr BP, suggesting the primary productivity increased during the later depositional episode of S1 (Aksu et al., 1999). Two reasons could explain the improvement of marine productivity: 1. The Mediterranean saltwater pours into the SoM, displacing the less-dense nutrient-rich bottom lacustrine water upward into the photic zone, which facilitates the primary productivity (Çağatay et al., 2009). 2. Riverine runoff mainly from the Black Sea provided phosphorus into surface waters, fueling diazotrophs and enhanced primary production (Castradori, 1993; Higgins et al., 2010; Sancetta, 1994; Vidal et al., 2010). Moreover, the warm and humid climate during the Mid-Holocene would also contribute to establishing

330 highly productive conditions (Çağatay et al., 1999; Çağatay et al., 2015; Triantaphyllou et
331 al., 2014).

332 The C/N profile of the upper part of the main sapropel diverges considerably from
333 that of the synchronous Black Sea sediments, whereas the C/N profiles of the younger
334 sediments deposited in the SoM and the Black Sea during 5.9-4 ka BP are more
335 conformable (Fig. 2c). These C/N trends suggest that although the Black Sea had high
336 input of terrestrial organic matter during the deposition of the upper part of the main
337 sapropel in the SoM, this matter was not transported to the SoM, which is likely due to a
338 restricted Black Sea outflow in the SoM. On the contrary, a similarity between C/N profiles
339 of the SoM and Black Sea sedimentary successions deposited during 5.9-4 ka BP interval
340 might suggest a strong Black Sea influence on the organic matter composition of the SoM.

341 The discussion above supports a model in which riverine runoff from the Black Sea
342 brings the terrestrial organic matter to the SoM, contributing to the earlier part of the main
343 sapropel deposition. The contribution of terrestrial fraction decreased, and marine primary
344 productivity increased in the SoM with time, ending with organic matter of predominantly
345 marine origin in the upper sapropel unit (see discussion in section 4.3 on
346 paleoceanographic scenarios).

347 **4.2 Redox conditions of sapropel deposition in the SoM: insights from nitrogen**
348 **utilization**

349 4.2.1 Lower part of the main (early Holocene) sapropel

350 The $\delta^{15}N$ ranges from 3.6‰ to 5.5‰ in the lower portion of the main sapropel
351 (Fig.3), which is higher than those in the overlying sediments. These positive values
352 indicate that the primary producers may have assimilated nitrogen induced by water

353 column denitrification that occurred under relatively suboxic-dysoxic conditions.
354 Denitrification is the process by which nitrate is reduced to N_2 or N_2O under suboxic
355 conditions (oxygen concentration < 5μM) (Sigman and Casciotti, 2009). The consumption
356 of nitrate through denitrification would leave the remaining nitrate pool enriched in ^{15}N
357 (Cremonese et al., 2013; Kikumoto et al., 2014; Sigman and Casciotti, 2009; Wang et al.,
358 2013). Thus the positive $\delta^{15}N$ values recorded in sedimentary organic matter indicate a
359 suboxic-dysoxic environment. In such an environment, the oxygen content is not high
360 enough to increase the nitrate supply to the organic nitrogen pool via oxidation. Therefore
361 the ^{15}N-rich nitrate is mostly preserved in the sediments (Kikumoto et al., 2014; Sigman
362 and Casciotti, 2009) (Fig.6a). In conclusion, the positive $\delta^{15}N$ signals in the early Holocene
363 sediments of the SoM generally reflect an oxygen-depleted bottom water condition. Lack
364 of oxygen penetration in sediments is supported by the independent observation of Mo
365 enrichment above crustal values of 2 ppm (Taylor and McLennan, 1985)(Fig. 3). In anoxic
366 and organic-rich sediments, Mo is rapidly sequestered into the organic and clay fractions
367 and precipitated as authigenic sulfide minerals where [H_2S_{aq}] reaches ~10μM (Helz et al.,
368 2011; Helz et al., 1996; Scott and Lyons, 2012). The Mo enrichment in core MD01-2430 in
369 the SoM also documented an anoxic condition during deposition of the lower part of the
370 main sapropel (Vidal et al., 2010). In addition, the scarcity of benthic foraminifera and
371 sporadic occurrences of dysoxic species were observed in the core MAR98-12 for the
372 same stratigraphic interval (Aksu et al., 2002).

373 4.2.2 Upper part of the main sapropel and the upper sapropel

374 The $\delta^{15}N$ remains low with an average value of 2.9‰ throughout the upper part of
375 the main sapropel and the upper sapropel units (895-680, 580-410 cmbsf) but drop to 2.3‰

376 at 4.10 mbsf. Depleted $\delta^{15}N$ signals are commonly attributed to either enhanced nitrate
377 supply or improved N_2 fixation (Kikumoto et al., 2014; Sigman and Casciotti, 2009). The
378 two hypotheses reconcile with previously discussed scenarios of improved marine
379 productivity. In scenarios 1, as dense Mediterranean water flows into the SoM and
380 displaces the less dense lake water, weak ventilation of the SoM is established (Çağatay et
381 al., 1999; Çağatay et al., 2009). The ventilation results in the oxidation of the organic
382 nitrogen pool, which leads to a gradual increase of nitrate reservoir. In a nitrate available
383 condition, partial assimilation of nitrate preferentially produces depleted $\delta^{15}N$ signals
384 (Kikumoto et al., 2014; Sigman and Casciotti, 2009). In the second scenario, increasing
385 river input from the Black Sea yields phosphate excess in the surface water, which
386 stimulates the diazotrophic N_2 fixation. The fixed nitrogen carries a $\delta^{15}N$ value of ~0‰
387 and then decreases the organic $\delta^{15}N$ values (Ader et al., 2014; Kikumoto et al., 2014; Sachs
388 and Repeta, 1999). Further decreased $\delta^{15}N$ values in the upper sapropel sediments would
389 reflect an integrated $\delta^{15}N$ signal of incomplete utilization of nitrate and nitrogen fixation.

390 Relative Mn enrichment in the upper part of the main sapropel and the upper
391 sapropel suggests improved bottom water ventilation (Fig.3). Mn, as a redox-sensitive
392 element, occurs in high concentrations as insoluble Mn-oxyhydroxides in the sediments
393 deposited under oxic bottom waters (Çağatay et al., 2002; Çağatay et al., 2004; Calvert and
394 Pedersen, 1993). Near the top of the main sapropel unit in core MAR98-12 in the Sea of
395 Marmara, the bloom in *Globobulimina* also indicates an improvement in deep water
396 oxygenation (Aksu et al., 2002). A similar observation of Mn peaks coinciding with the
397 benthic foraminiferal record (*G.orbicularis*) in sapropel S1 was previously made and

Journal Pre-proof

398 interpreted to be indicative of increased deepwater ventilation in the Mediterranean Sea
399 (Mercone et al., 2001).

400 **4.3 Paleoceanographic scenarios of sapropel deposition**

401 Riverine runoff from the Black Sea transferred into the SoM from the Late Glacial
402 until the end of the Younger Dryas (Eriş et al., 2007; Vidal et al., 2010), which induced
403 low-salinity surface water and a high input of terrestrial organic matter (Fig.6a). At about
404 12.6 kyr BP, the SoM was reconnected with the Mediterranean Sea (Çağatay et al., 2015).
405 Subsequently, a salinity stratification was established with the saline Mediterranean waters
406 below and the brackish-fresh lacustrine of the Marmara Lake waters above (Çağatay et al.,
407 2000)(Fig.6a). The density stratification prevented deepwater ventilation and oxygen
408 supply to the bottom waters (Aksu et al., 1999; Çağatay et al., 2000; Tolun et al., 2002).
409 After the Younger Dryas, the water level of the Black Sea dropped below the Bosporus sill
410 for a short period because of a decrease in precipitation (Ryan, 2007). This disconnection
411 was supported by a salinity increase in the surface water of the SoM (an increment of about
412 2.5 ‰ in $\Delta\delta^{18}O_{sw}$) (Vidal et al., 2010).

413 The SoM was reconnected with the Black Sea with the overspill of Mediterranean
414 waters via the Bosporus at 9 ka BP (Major et al., 2006; Ryan, 2007; Soulet et al., 2011).
415 The main sapropel was deposited shortly after this reconnection, and the Black Sea's
416 outflow caused a decrease in the surface salinity of the SoM during the sapropel
417 deposition (Sperling et al., 2003; Vidal et al., 2010) (Fig. 6b), while the continuous dense
418 Mediterranean seawater poured into the SoM and caused ventilation (Fig. 6b). The
419 outflow from the Black Sea was weakened at ~ 6.5 kyr BP as indicated by surface salinity
420 increase in the SoM (Hiscott and Aksu, 2002), and the main Holocene sapropel

421 deposition ceased soon afterward (~ 6 kyr BP) (Çağatay et al., 2015; Hiscott and Aksu,
422 2002; Sperling et al., 2003).

423 The upper sapropel deposition took place between ~5.4 to ~3 kyr BP (Çağatay et
424 al., 2015), when there was a warm and humid mid-Holocene episode in the region
425 (Triantaphyllou et al. 2014; Çağatay et al., 2015). The start of the upper sapropel deposition
426 also coincided with the establishment of the present-day layer flow system in the Bosporus
427 Strait and the SoM (Algan et al., 2001; Çağatay et al., 2000; Fontanier et al., 2018) (Fig. 6c).
428 The warm and humid conditions resulted from the albeit weak Mid-Holocene South
429 Asian monsoon forcing and the lighter Etesian wind (Triantaphyllou et al., 2014),
430 resulting in a relatively slow bottom water circulation and stagnation, leading to the
431 deposition of the upper sapropel.

432 An interruption in organic-rich sediment deposition occurred between the two
433 sapropel layers (Fig.1), which show conformable negative excursions in the TOC and TN
434 contents (Fig.2). Poor sorting and positively skewed grain size distribution, together with
435 the coarser mean grain size in the interval between the two sapropels, imply an interruption
436 of uniform sedimentation, which was likely caused by increased deepwater circulation
437 (Fig.4). The upper sapropelic unit, with fine grain size and improved sorting, was
438 deposited during a high stand of global sea level similar to the present day level.

Journal Pre-proof

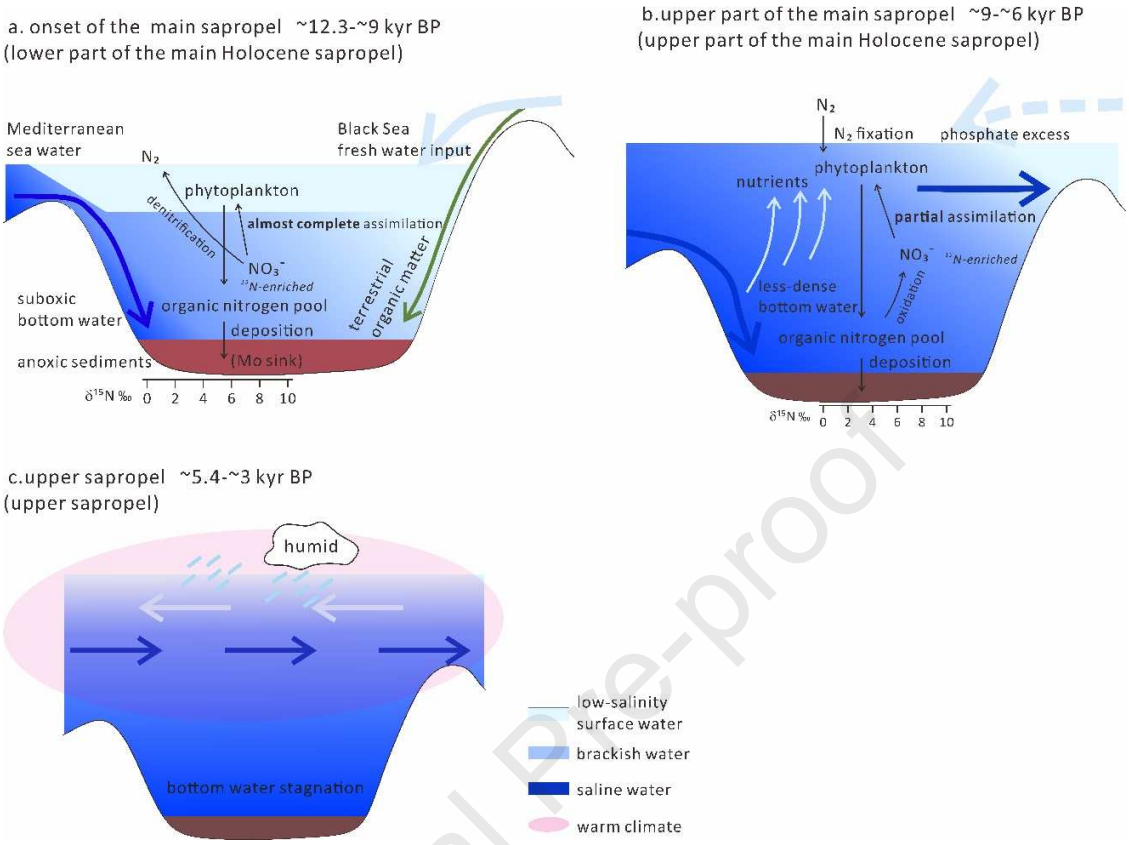

Figure 6. Paleo-hydrological models showing the ocean redox structure and nitrogen utilization during the sapropel formation in the SoM. (a) The main Holocene sapropel started depositing at 12.3 kyr BP, about 300 years after the Mediterranean transgression (Çağatay et al., 2015). The lower part of the main Marmara sapropel was deposited during the Younger Dryas until the inflow of Black Sea waters in the SoM ceased. However, Core MRS-CS 17 fails to capture this period as it extends back to ~8 ka BP, and thus the scenario for this period is hypothetical. The salinity gradient between the saline Mediterranean seawater and the fresh-brackish lacustrine water during this early period resulted in a strong stratification of the water column in the SoM. Anoxic conditions were established in a mode similar to the present-day Black Sea. With no or little oxygen, no nitrification through the oxidation of the organic nitrogen pool was possible. (b) An increase in the bottom water ventilation of the SoM started when the dense Mediterranean seawater began pouring into the Black Sea at ~9 kyr BP. The ventilation caused the oxidation of the organic nitrogen pool and resulting in a gradual increase in the nitrate reservoir. The ventilation weakened with the rise of the global sea level to its present position at ~6.5 kyr. Freshwater input with phosphate excess in the surface seawater may have stimulated the diazotrophic N_2 fixation during this period. (c). After the establishment of the present two-way flow system between the Mediterranean and Black Sea waters, the upper sapropel started depositing between ~5.4 to ~3 kyr BP during a warm and humid climatic period. These climatic conditions resulted in enhanced productivity and relatively slow bottom water circulation and stagnation.

5 Conclusions

Multi-proxies from core MRS-CS 17 retrieved in the SoM provide paleoenvironmental and hydrographic information reaching back to the early Holocene. The C/N ratios and $\delta^{13}C_{org}$ values show that most of the organic carbon at the onset of the lower sapropel is of terrestrial origin, and then the marine productivity contribution increased upward. Isotope analyses of total nitrogen suggest relatively high $\delta^{15}N$ up to 5.5 ‰ at the bottom, and then it dropped to around 2.9 ‰ in the upper sapropel. The variation can be viewed as a shift in nutrient condition from a nitrate-limited to a temporal nitrate-rich one due to a gradual increase in the bottom water oxygen concentrations. This hypothesis is supported by redox-sensitive elements (Mo and Mn), which indicate anoxic conditions when the main sapropel was deposited, and then deepwater ventilation was strengthened and water O_2 levels was increased when the upper sapropel was formed.

This research attempts to further understand the relationship between the Holocene sapropel deposition in the SoM and the regional paleo-hydrological conditions. During the deposition of the lower part of the main Holocene sapropel, which started at ~12.3 kyr BP, the density stratification between brackish-fresh lacustrine and the saline Mediterranean water prevented deepwater ventilation and oxygen supply to bottom water. As a result, the lower part of the main sapropel was deposited under suboxic/anoxic bottom water. The terrestrial organic matter in the lower part of the main Holocene sapropel was mainly provided by organic-laden riverine runoff from the Black Sea (Çağatay et al., 2009; Çağatay et al., 2000; Tolun et al., 2002). After the Younger Dryas, the outflow from the Black Sea ceased for a short period. As the dense Mediterranean seawater continued to pour into the SoM, it displaced less-dense, nutrient-rich lake

Journal Pre-proof

bottom waters upward to the surface, which leads to water stratification and bottom water anoxia/hypoxia, and finally to the main Holocene sapropel deposition. Later ventilation might have improved the oxygen-level, leading to a gradual increase of nitrate reservoir after the Mediterranean reconnection of the Black Sea at ca. 9 kyr BP. An outflow of the Black Sea to the SoM also started soon after the ingression of Mediterranean waters in the Black Sea. The river flow related phosphorus excess from the Balck Sea could have prompted nitrogen fixation in the SoM. The phosphorus-rich surface water and the upward nutrient-rich bottom lacustrine water facilitated the enhanced marine productivity in the upper part of the main sapropel. The upper sapropel deposition occurred in a warm and humid mid to late Holocene period between ~5.4 and ~3 kyr BP. These climatic conditions resulted in relatively slow bottom water circulation and enhanced organic productivity.

Acknowledgments

We appreciate the captain and his crew onboard the *RV Pourquoi pas*? and onboard scientists for their support in sampling. All data are included in the supporting information. The financial supports, 2017YFC0307603 from the Ministry of Science and Technology of the People's Republic of China, and DD20190234 and HD-JJHT-20 from China Geological Survey, to HL made this research possible. We would like to express our gratitude to the editor and anonymous reviewers for their constructive comments and suggestions.

References

Ader, M., Sansjofre, P., Halverson, G.P., Busigny, V., Trindade, R.I.F., Kunzmann, M., Nogueira, A.C.R., 2014. Ocean redox structure across the Late Neoproterozoic Oxygenation Event: A nitrogen isotope perspective. Earth & Planetary Science Letters 396, 1-13.

Aksu, A.E., Abrajano, T., Mudie, P.J., Yaşar, D., 1999. Organic geochemical and palynological evidence for terrigenous origin of the organic matter in Aegean Sea sapropel S1. Marine Geology 153, 303-318.

Aksu, A.E., Hiscott, R.N., Kaminski, M.A., Mudie, P.J., Gillespie, H., Abrajano, T., Yaşar, D., 2002. Last glacial-Holocene paleoceanography of the Black Sea and Marmara Sea: stable isotopic, foraminiferal and coccolith evidence. Marine Geology 190, 119-149.

Algan, O., Çağatay, N., Chepalyga, A., Ongan, D., Eastoe, C., Gökaşan, E., 2001. Stratigraphy of the sediment infill in Bosphorus Strait: water exchange between the Black and Mediterranean Seas during the last glacial Holocene. Geo-Marine Letters 20, 209-218.

Bahr, A., Lamy, F., Arz, H., Kuhlmann, H., Wefer, G., 2005. Late glacial to Holocene climate and sedimentation history in the NW Black Sea. Marine Geology 214, 309-322.

Benkovitz, A., Matthews, A., Teutsch, N., Poulton, S.W., Bar-Matthews, M., Almogi-Labin, A., 2020. Tracing water column euxinia in Eastern Mediterranean Sapropels S5 and S7. Chemical Geology 545.

Bouloubassi, I., Rullkötter, J., Meyers, P.A., 1999. Origin and transformation of organic matter in Pliocene-Pleistocene Mediterranean sapropels: organic geochemical evidence reviewed. Marine Geology 153, 177-197.

Brunner, B., Contreras, S., Lehmann, M.F., Matantseva, O., Rollog, M., Kalvelage, T., Klockgether, G., Lavik, G., Jetten, M.S.M., Kartal, B., Kuypers, M.M.M., 2013. Nitrogen isotope effects induced by anammox bacteria. Proceedings of the National Academy of Sciences 110, 18994-18999.

Çağatay, M.N., Algan, O., Sakınç, M., Eastoe, C.J., Egesel, L., Balkis, N., Ongan, D., Caner, H., 1999. A mid-late Holocene sapropelic sediment unit from the southern Marmara sea shelf and its palaeoceanographic significance. Quaternary Science Reviews 18, 531-540.

Çağatay, M.N., Erel, L., Bellucci, L.G., Polonia, A., Gasperini, L., Eriş, K.K., Sancar, Ü., Biltekin, D., Uçarkuş, G., Ülgen, U.B., Damcı, E., 2012. Sedimentary earthquake records in the İzmit Gulf, Sea of Marmara, Turkey. Sedimentary Geology 282, 347-359.

Çağatay, M.N., EriŞ, K., Makaroğlu, Ö., Yakupoğlu, N., Henry, P., Leroy, S., Ucarkus, G., Sakınç, M., Yalamaz, B., Bozyiğit, C., Kende, J., 2019. The Sea of Marmara during Marine Isotope Stages 5 and 6. Quaternary Science Reviews 220, 124-141.

Çağatay, M.N., Eriş, K., Ryan, W.B.F., Sancar, Ü., Polonia, A., Akçer, S., Biltekin, D., Gasperini, L., Görür, N., Lericolais, G., Bard, E., 2009. Late Pleistocene–Holocene evolution of the northern shelf of the Sea of Marmara. Marine Geology 265, 87-100.

Çağatay, M.N., Görür, N., Algan, O., Eastoe, C., Tchapalyga, A., Ongan, D., Kuhn, T., Kuşcu, I., 2000. Late Glacial–Holocene palaeoceanography of the Sea of Marmara: timing of connections with the Mediterranean and the Black Seas. Marine Geology 167, 191-206.

Çağatay, M.N., Keigwin, L.D., Okay, N., Sarı, E., Algan, O., 2002. Variability of clay-mineral composition on Carolina Slope (NW Atlantic) during marine isotope stages 1-3 and its paleoceanographic significance. Marine Geology 189, 163-174.

Journal Pre-proof

546 Çağatay, M.N., Özcan, M., Güngör, E., 2004. Pore-water and sediment geochemistry in the
547 Marmara Sea (Turkey): Early diagenesis and diffusive fluxes. Geochemistry: Exploration,
548 Environment, Analysis 4, 213-225.
549 Çağatay, M.N., Wulf, S., Sancar, Ü., Özmaral, A., Vidal, L., Henry, P., Appelt, O., Gasperini, L.,
550 2015. The tephra record from the Sea of Marmara for the last ca. 70 ka and its palaeoceanographic
551 implications. Marine Geology 361, 96-110.
552 Calvert, S.E., 2004. Beware intercepts: interpreting compositional ratios in multi-component
553 sediments and sedimentary rocks. Organic Geochemistry 35, 981-987.
554 Calvert, S.E., Fontugne, M.R., 1987. Stable carbon isotopic evidence for the marine origin of the
555 organic matter in the holocene black sea sapropel. Chemical Geology: Isotope Geoscience section
556 66, 315-322.
557 Calvert, S.E., Nielsen, B., Fontugne, M.R., 1992. Evidence from nitrogen isotope ratios for
558 enhanced productivity during formation of eastern Mediterranean sapropels. Nature 359, 223-225.
559 Calvert, S.E., Pedersen, T.F., 1993. Geochemistry of Recent oxic and anoxic marine sediments:
560 Implications for the geological record. Marine Geology 113, 67-88.
561 Canfield, D.E., Glazer, A.N., Falkowski, P.G., 2010. The evolution and future of Earth's nitrogen
562 cycle. Science 330, 192-196.
563 Castradori, D., 1993. Calcareous nannofossils and the origin of eastern Mediterranean sapropels.
564 Paleoceanography 8, 459-471.
565 Checa, H., Margaritelli, G., Pena, L.D., Frigola, J., Cacho, I., Rettori, R., Lirer, F., 2020. High
566 resolution paleoenvironmental changes during the Sapropel 1 in the North Ionian Sea, central
567 Mediterranean. The Holocene 30, 1504-1515.
568 Cremonese, L., Shields-Zhou, G., Struck, U., Ling, H.F., Och, L., Chen, X., Li, D., 2013. Marine
569 biogeochemical cycling during the early Cambrian constrained by a nitrogen and organic carbon
570 isotope study of the Xiaotan section, South China. Precambrian Research 225, 148-165.
571 De Lange, G.J., Thomson, J., Reitz, A., Slomp, C.P., Speranza Principato, M., Erba, E., Corselli, C.,
572 2008. Synchronous basin-wide formation and redox-controlled preservation of a Mediterranean
573 sapropel. Nature Geoscience 1, 606-610.
574 Dirksen, J.P., Hennekam, R., Geerken, E., Reichart, G.J., 2019. A Novel Approach Using Time-
575 Depth Distortions to Assess Multicentennial Variability in Deep-Sea Oxygen Deficiency in the
576 Eastern Mediterranean Sea During Sapropel S5. Paleoceanography and Paleoclimatology 34,
577 774-786.
578 Dirksen, J.P., Meijer, P., 2020. The mechanism of sapropel formation in the Mediterranean Sea:
579 insight from long-duration box model experiments. Climate of the Past 16, 933-952.
580 Emerson, S., Hedges, J.I., 1988. Processes controlling the organic carbon content of open ocean
581 sediments. Paleoceanography 3, 621-634.

Journal Pre-proof

582 Eriş, K.K., Ryan, W.B.F., Çağatay, M.N., Sancar, U., Lericolais, G., Ménot, G., Bard, E., 2007. The
583 timing and evolution of the post-glacial transgression across the Sea of Marmara shelf south of
584 İstanbul. Marine Geology 243, 57-76.
585 Fontanier, C., Dissard, D., Ruffine, L., Mamo, B., Ponzevera, E., Pelleter, E., Baudin, F., Roubi, A.,
586 Chéron, S., Boissier, A., Gayet, N., Bermell-Fleury, S., Pitel, M., Guyader, V., Lesongeur, F.,
587 Savignac, F., 2018. Living (stained) deep-sea foraminifera from the Sea of Marmara: A preliminary
588 study. Deep Sea Research Part II: Topical Studies in Oceanography 153, 61-78.
589 Francis, C.A., Beman, J.M., Kuypers, M.M.M., 2007. New processes and players in the nitrogen
590 cycle: the microbial ecology of anaerobic and archaeal ammonia oxidation. The ISME Journal 1,
591 19-27.
592 Fulton, J.M., Arthur, M.A., Freeman, K.H., 2012. Black Sea nitrogen cycling and the preservation of
593 phytoplankton d 15 N signals during the Holocene. Global Biogeochemical Cycles 26.
594 Grant, K.M., Grimm, R., Mikolajewicz, U., Marino, G., Ziegler, M., Rohling, E.J., 2016. The timing of
595 Mediterranean sapropel deposition relative to insolation, sea-level and African monsoon changes.
596 Quaternary Science Reviews 140, 125-141.
597 Grimm, R., Maier-Reimer, E., Mikolajewicz, U., Schmiedl, G., Müller-Navarra, K., Adloff, F., Grant,
598 K.M., Ziegler, M., Lourens, L.J., Emeis, K.-C., 2015. Late glacial initiation of Holocene eastern
599 Mediterranean sapropel formation. Nature Communications 6, 7099.
600 Helz, G.R., Bura-Nakić, E., Mikac, N., Ciglenečki, I., 2011. New model for molybdenum behavior in
601 euxinic waters. Chemical Geology 284, 323-332.
602 Helz, G.R., Miller, C.V., Charnock, J.M., Mosselmans, J.F.W., Pattrick, R.A.D., Garner, C.D.,
603 Vaughan, D.J., 1996. Mechanism of molybdenum removal from the sea and its concentration in
604 black shales: EXAFS evidence. Geochimica Et Cosmochimica Acta 60, 0-3642.
605 Higgins, M.B., Robinson, R.S., Carter, S.J., Pearson, A., 2010. Evidence from chlorin nitrogen
606 isotopes for alternating nutrient regimes in the Eastern Mediterranean Sea. Earth and Planetary
607 Science Letters 290, 102-107.
608 Hiscott, R.N., Aksu, A.E., 2002. Late Quaternary history of the Marmara Sea and Black Sea from
609 high-resolution seismic and gravity-core studies. Marine Geology 190, 261-282.
610 Holmes, M.E., Eichner, C., Struck, U., Wefer, G., 1999. Reconstruction of Surface Ocean Nitrate
611 Utilization Using Stable Nitrogen Isotopes in Sinking Particles and Sediments, in: Fischerr, G.,
612 Wefer, G. (Eds.), Use of Proxies in Palaeoceanography: Examples From the South Atlantic.
613 Springer-Verlag, New York, pp. 447-468.
614 Kikumoto, R., Tahata, M., Nishizawa, M., Sawaki, Y., Maruyama, S., Shu, D., Han, J., Komiya, T.,
615 Takai, K., Ueno, Y., 2014. Nitrogen isotope chemostratigraphy of the Ediacaran and Early
616 Cambrian platform sequence at Three Gorges, South China. Gondwana Research 25, 1057-1069.
617 Kirci-Elmas, E., Algan, O., Özkar-Öngen, Z., Altenbach, A.V., Sagular, S.K., Struck, U., 2008.
618 Palaeoenvironmental Investigation of Sapropelic Sediments from the Marmara Sea: A

Biostratigraphic Approach to Palaeoceanographic History During the Last Glacial-Holocene. Turkish Journal of Earth Sciences 17, 129-168.

Lane-Serff, G.F., Rohling, E.J., Bryden, H.L., Charnock, H., 1997. Postglacial connection of the Black Sea to the Mediterranean and its relation to the timing of sapropel formation. Paleoceanography 12, 169-174.

Liu, Y., Lu, H., Yin, X., Ruffine, L., Çağatay, M.N., Yang, H., Chen, C., He, D., Zhu, Z., Yalamaz, B., 2019. Interpretation of Late-Pleistocene/Holocene Transition in the Sea of Marmara From Geochemistry of Bulk Carbonates. Geochemistry, Geophysics, Geosystems 20, 4487-4504.

Major, C.O., Goldstein, S.L., Ryan, W.B.F., Lericolais, G., Piotrowski, A.M., Hajdas, I., 2006. The co-evolution of Black Sea level and composition through the last deglaciation and its paleoclimatic significance. Quaternary Science Reviews 25, 2031-2047.

Mercone, D., Thomson, J., Abu-Zied, R.H., Croudace, I.W., Rohling, E.J., 2001. High-resolution geochemical and micropalaeontological proifling of the most recent eastern Mediterranean sapropel. Marine Geology 177, 25-44.

Möbius, J., Lahajnar, N., Emeis, K.C., 2010. Diagenetic control of nitrogen isotope ratios in Holocene sapropels and recent sediments from the Eastern Mediterranean Sea. Biogeosciences 7, 3901-3914.

Montoya, J.P., Voss, M., 2006. Nitrogen Cycling in Suboxicwaters: Isotopic Signatures of Nitrogen Transformation in the Arabian Sea Oxygen Minimum Zone, Past and Present Water Column Anoxia, pp. 257-281.

Moodley, L., Middelburg, J.J., Herman, P.M.J., Soetaert, K., de Lange, G.J., 2005. Oxygenation and organic-matter preservation in marine sediments: Direct experimental evidence from ancient organic carbon-rich deposits. Geology 33, 889-892.

Reimer, P.J., Bard, E., Bayliss, A., Beck, J.W., Blackwell, P.G., Ramsey, C.B., Buck, C.E., Cheng, H., Edwards, R.L., Friedrich, M., Grootes, P.M., Guilderson, T.P., Haflidason, H., Hajdas, I., Hatté, C., Heaton, T.J., Hoffmann, D.L., Hogg, A.G., Hughen, K.A., Kaiser, K.F., Kromer, B., Manning, S.W., Niu, M., Reimer, R.W., Richards, D.A., Scott, E.M., Southon, J.R., Staff, R.A., Turney, C.S.M., van der Plicht, J., 2013. IntCal09 and Marine09 radiocarbon age Calibration Curves, 0-50,000 Years cal BP. Radiocarbon 51, 1869-1887.

Robinson, R.S., Kienast, M., Luiza Albuquerque, A., Altabet, M., Contreras, S., De Pol Holz, R., Dubois, N., Francois, R., Galbraith, E., Hsu, T.-C., Ivanochko, T., Jaccard, S., Kao, S.-J., Kiefer, T., Kienast, S., Lehmann, M., Martinez, P., McCarthy, M., Möbius, J., Pedersen, T., Quan, T.M., Ryabenko, E., Schmittner, A., Schneider, R., Schneider-Mor, A., Shigemitsu, M., Sinclair, D., Somes, C., Studer, A., Thunell, R., Yang, J.-Y., 2012. A review of nitrogen isotopic alteration in marine sediments. Paleoceanography 27, PA4023.

Rohling, E.J., Marino, G., Grant, K.M., 2015. Mediterranean climate and oceanography, and the periodic development of anoxic events (sapropels). Earth-Science Reviews 143, 62-97.

Ryan, W.B.F., 2007. Status of the Black Sea flood hypothesis, The Black Sea Flood Question: Changes in Coastline, Climate, and Human Settlement, pp. 63-88.

Sachs, J.P., Repeta, D.J., 1999. Oligotrophy and Nitrogen Fixation During Eastern Mediterranean Sapropel Events. Science 286, 2485-2488.

Sancetta, C., 1994. Mediterranean sapropels: seasonal stratification yields high production and carbon flux. Paleoceanography 9, 195-196.

Scott, C., Lyons, T.W., 2012. Contrasting molybdenum cycling and isotopic properties in euxinic versus non-euxinic sediments and sedimentary rocks: Refining the paleoproxies. Chemical Geology 324-325, 19-27.

Siani, G., Paterne, M., Arnold, M., Bard, E., Métivier, B., Tisnerat, N., Bassinot, F., 2000. Radiocarbon reservoir ages in the Mediterranean Sea and Black Sea. Radiocarbon 42, 271-280.

Sigman, D.M., Altabet, M.A., Mccorkle, D.C., Francois, R., Fischer, G., 2000. The δ15N of nitrate in the Southern Ocean: Nitrogen cycling and circulation in the ocean interior. Journal of Geophysical Research Atmospheres 105, 19599-19614.

Sigman, D.M., Casciotti, K.L., 2009. Nitrogen Isotopes in the Ocean, in: Steele, J.H. (Ed.), Encyclopedia of Ocean Sciences (Second Edition). Academic Press, pp. 40-54.

Soulet, G., Ménot, G., Garreta, V., Rostek, F., Zaragosi, S., Lericolais, G., Bard, E., 2011. Black Sea "Lake" reservoir age evolution since the Last Glacial-Hydrologic and climatic implications. Earth & Planetary Science Letters 308, 245-258.

Sperling, M., Schmiedl, G., Hemleben, C., Emeis, K.C., Erlenkeuser, H., Grootes, P.M., 2003. Black Sea impact on the formation of eastern Mediterranean sapropel S1? Evidence from the Marmara Sea. Palaeogeography Palaeoclimatology Palaeoecology 190, 9-21.

Stüeken, E.E., Kipp, M.A., Koehler, M.C., Buick, R., 2016. The evolution of Earth's biogeochemical nitrogen cycle. Earth-Science Reviews 160, 220-239.

Taylor, S.R., McLennan, S.M., 1985. in: Blackwell (Ed.), The Continental Crust: Its Composition and Evolution., Oxford, p. 312.

Tolun, L., Çağatay, M.N., Carrigan, W.J., 2002. Organic geochemistry and origin of Late Glacial–Holocene sapropelic layers and associated sediments in Marmara Sea. Marine Geology 190, 47-60.

Triantaphyllou, M.V., Gogou, A., Bouloubassi, I., Dimiza, M., Kouli, K., Rousakis, G., Kotthoff, U., Emeis, K.C., Papanikolaou, M., Athanasiou, M., Parinos, C., Ioakim, C., Lykousis, V., 2014. Evidence for a warm and humid Mid-Holocene episode in the Aegean and northern Levantine Seas (Greece, NE Mediterranean). Regional Environmental Change 14, 1697-1712.

Vidal, L., Ménot, G., Joly, C., Bruneton, H., Rostek, F., Ccedil, Ağatay, M.N., Major, C., Bard, E., 2010. Hydrology in the Sea of Marmara during the last 23 ka: Implications for timing of Black Sea connections and sapropel deposition. Paleoceanography 25, 1205.

692 Wang, D., Ling, H.F., Struck, U., Zhu, X., Shields, G.A., 2018a. Coupling of ocean redox and animal
693 evolution during the Ediacaran-Cambrian transition. Nature Communications 9, 1-8.
694 Wang, X., Jiang, G., Shi, X., Peng, Y., Morales, D.C., 2018b. Nitrogen isotope constraints on the
695 early Ediacaran ocean redox structure. Geochimica et Cosmochimica Acta 240, 220-235.
696 Wang, X., Shi, X., Tang, D., Zhang, W., 2013. Nitrogen Isotope Evidence for Redox Variations at
697 the Ediacaran-Cambrian Transition in South China. The Journal of Geology 121, 489-502.
698 Wei, G., Ling, H.-F., Li, D., Wei, W., Wang, D., Chen, X., Zhu, X., Zhang, F., Yan, B., 2017. Marine
699 redox evolution in the early Cambrian Yangtze shelf margin area: evidence from trace elements,
700 nitrogen and sulphur isotopes. Geological Magazine 154, 1344-1359.
701 Wei, W., Wang, D., Li, D., Ling, H.-F., Chen, X., Wei, G., Zhang, F., Zhu, X., Yan, B., 2016. The
702 marine redox change and nitrogen cycle in the Early Cryogenian interglacial time: Evidence from
703 nitrogen isotopes and Mo contents of the basal Datangpo Formation, northeastern Guizhou, South
704 China. Journal of Earth Science 27, 233-241.
705

Journal Pre-proof

Journal Pre-proof

Highlights

1. Nitrogen isotopic compositions in the Holocene sapropels from the Sea of the Marmara are reported for the first time to reconstruct paleoceanographic conditions.
2. The redox condition changed from suboxic-dysoxic to relatively oxidative during the Holocene sapropel deposition in the Sea of Marmara.
3. The nutrition condition shifted from low nitrate to temporally nitrate-rich due to a gradual increase in the bottom water oxygen concentration during the sapropel deposition.
4. Holocene sapropel deposition in the Sea of Marmara was closely related to the regional paleo-hydrological condition.

Journal Pre-proof

Journal Pre-proof

Declaration of interests

☒ The authors declare that they have no known competing financial interests or personal relationships that could have appeared to influence the work reported in this paper.

☐The authors declare the following financial interests/personal relationships which may be considered as potential competing interests:

Journal Pre-proof